Study of the Monochromator Shielding Block Redesign of the HANARO Cold Neutron Triple-Axis Spectrometer

Ji-Myung Ryu [a*], J. M. Sungil Park [a], Beak-Seok Seong [a]
[a]*Neutron Instrumentation Division, Korea Atomic Energy Research Institute*
[*]*Corresponding author: jmryu@kaeri.re.kr*

1. Introduction

The cold neutron triple-axis spectrometer (Cold-TAS) at HANARO, which is designed for low energy inelastic neutron scattering, is undergoing a heavy reconstruction of its monochromator shielding blocks to augment their structural integrity. The monochromator shielding consists of the segmented shielding for the beam path opening and the concrete shielding that gives the structural support to the former. The segmented shielding is made of 17 segments of boron-added polyethylene and lead and originally weighed 4.6 tons in total. The center of gravity of the segmented shielding is 70 cm from the monochromator axis exerting a large amount of force to the supporting concrete shielding blocks, which are made of stainless-steel-casemated heavy concrete of varying densities. Among the several concrete shielding blocks, the four vertically standing ones bear most of the weight of the segmented shielding and have shown signs of deformation. The segmented shielding was later modified to relieve the strain and the total weight became 2.7 tons. [1, 2] (Fig. 1)

Fig. 1. Cold Neutron Triple-Axis Spectrometer and its modified monochromator shielding at HANARO

Even after the modification, the four concrete blocks continually deformed. Taking advantage of the long shutdown of the reactor, it was decided to revamp the monochromator shielding to ensure future safety. While this work would not change the overall shape very much, we decided to use this opportunity to strengthen the shielding by means of clever redesign using MCNP calculations. Assuming a point neutron source at the monochromator location, it was found that most of the radiation outside the shielding blocks passes through the polyethylene parts of the segmented shielding and that it can be effectively suppressed by adding the thin metallic shielding on top of the polyethylene. [3]

2. Methods and Results

In this section, the details of the MCNP calculations are given starting with the description of the materials of the shielding blocks and the neutron source. For the MCNP calculations, MCNP6 package was used. We could observe the change of the neutron and gamma flux distribution as the shielding block design was improved. Mesh size of the flux distribution is 2 cm along the y and z axis and error was under 10% with excess of 1,000 particles per second per square centimeters.

2.1 Materials of the shielding blocks

Heavy concrete, lead and boron-added polyethylene are mainly used materials for the monochromator shielding. Heavy concrete had the density of 3.4 g/cm^3 previously. It was changed to 4.0 g/cm^3 in the redesign. Although lead with a trace amount of impurity such as tungsten was used for the segmented shielding to stop secondary radiation, pure lead was used for the calculation for simplicity. The boron content in polyethylene is 5% and remained unchanged. The stainless steel casemates were not simulated.

2.2 Definition of the neutron source

Cold neutrons are generated by the cold neutron source (CNS) in the reflector tank of the reactor. They are transferred to the neutron instrument through the supermirror coated cold neutron guide, CG5, for about 50 meters. In the downstream of the guide, the fast rotating mechanical filter, the neutron velocity selector (NVS), allows only a short band of neutron energies to pass through, thus reducing the cold neutron flux significantly. The beam is further monochromatized by using the crystalline monochromator made of pyrolithic graphite and sent to the sample being studied.

In this study we ignored the effect of the NVS and used the white beam instead. This will give us a very "conservative" estimate, but is good enough for comparing the different shielding designs. Accurate estimation of the radiation can be done by employing the filtered neutron beam by the NVS, but it will be the point of future study.

Unfortunately the MCNP alone cannot simulate all the way from the reactor to the instrument due to the long distance and the Bragg optics involved. In those cases, neutron beam simulators such as McStas is usually employed to bridge the reactor and the instrument. [4] McStas provides an efficient calculation of the neutron flux through the neutron guide, and the CG5 was successfully simulated. McStas produced the neutron flux at the monochromator position as a function of wavelength. We have converted the neutron flux data to the format suitable for MCNP calculations, i.e., flux as a function of neutron energies by using the simple conversion equation:

$$E = \frac{81.80}{\lambda^2} \qquad (1)$$

Where E is the neutron energy [meV] and λ is the neutron wavelength [Å]. Although it is not realistic, an isotropic source at the monochromator location was assumed to ensure that all part of the shielding is irradiated to suit our purpose.

2.3 Modification of shielding blocks

2.3.1 Segmented shielding

The existing segmented shielding effectively shields neutrons at the polyethylene parts close to the source (the origin in the figures) even when the segment is open as shown on the left sides of figure 1, and more so when the segment is closed on the left of figure 2. However, this geometry has a weakness in that gamma can penetrate the polyethylene upward where nothing blocks the high energy radiation other than the polyethylene as shown on the right sides of figures 1 and 2 for open and closed configurations respectively.

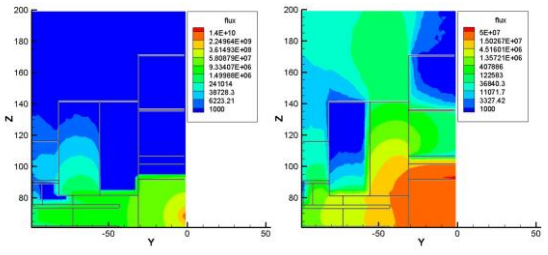

Fig. 1. Distribution of neutron and gamma flux with original segmented shielding blocks. (Open beam path)

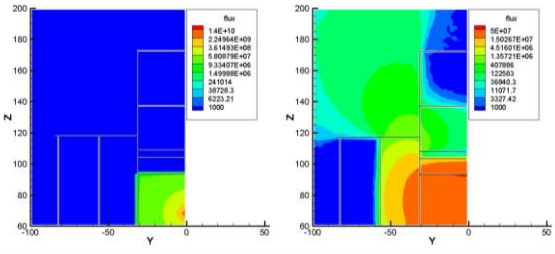

Fig. 2. Distribution of neutron and gamma flux with original segmented shielding blocks. (Closed beam path)

In order to reduce gamma leakage through the existing polyethylene parts, 5 cm thick lead plates were added on top of them for the next simulation. Neutron flux distribution for both open and closed beam paths is shown on the left sides of figure 3 and 4 respectively. It is essentially unchanged because the neutrons cannot reach the lead plates anyway. However, the gamma flux was reduced greatly thanks to the lead plate (right of figure 3 and 4). It was also identified that the current geometry allows gamma to bypass the newly placed lead plate and to scatter off from the top shielding blocks, resulting in higher gamma flux when the segmented shielding is closed (right of figure 4).

The Simple geometrical consideration would require a 20 cm thick plate instead of a 5 cm lead plate to eliminate the gamma leakage when the segment is open. Due to material properties, it is undesirable to machine 20 cm lead plates. Therefore, for the purpose of this simulation, 10 cm stainless steel was placed on top of 10 cm lead. As expected, gamma is almost completely stopped with this geometry with the beam is closed (figure 5). When the beam is open, it is now observable that scattered gamma leaks from the polyethylene into the top shielding above the monochromator.

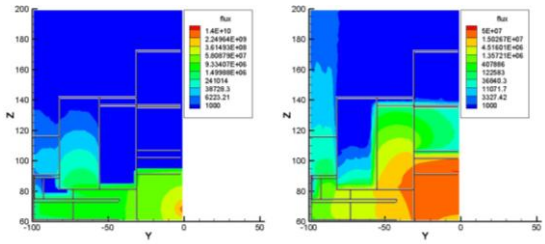

Fig. 3. Distribution of neutron and gamma flux with adding 5 cm lead on the top of segmented polyethylene. (Open beam path)

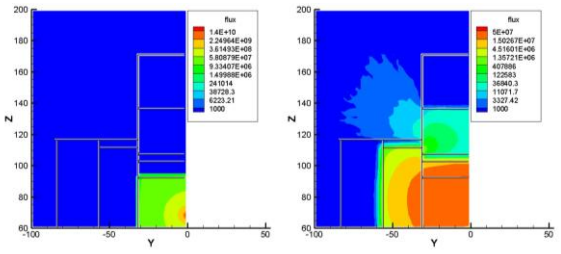

Fig. 4. Distribution of neutron and gamma flux with adding 5 cm lead on the top of segmented polyethylene. (Closed beam path)

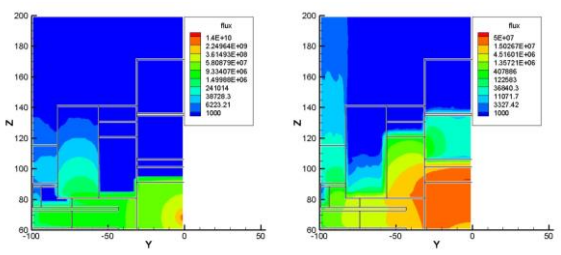

Fig. 5. Distribution of neutron and gamma flux with adding 10 cm lead and 10 cm stainless steel on the top of segmented polyethylene. (Open beam path)

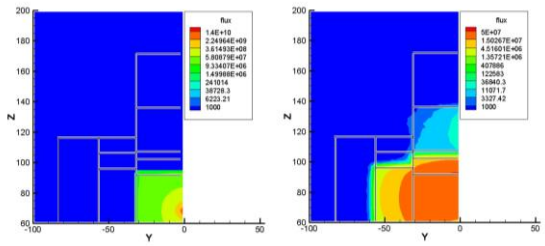

Fig. 6. Distribution of neutron and gamma flux with added 10 cm lead and 10 cm stainless steel on the top of segmented polyethylene. (Closed beam path)

2.3.2 Top shielding block above the monochromator

The top shielding block above the monochromator consists of 10 cm polyethylene at the bottom close to the monochromator, 5 cm lead, 25 cm polyethylene and 30 cm heavy concrete at the very top. Flux distribution of neutron and gamma radiation when the original shielding material was used is shown in figure 7. The polyethylene piece located at the back of the monochromator and the polyethylene in the middle of the top shielding block acted as a conduit of gamma radiation.

Material and thickness of the block was changed in the redesign for better shielding. Firstly the polyethylene at the bottom was changed from 10 cm to 5 cm, which is enough to shield low energy neutrons. The middle polyethylene was changed to heavy concrete to block gammas. More importantly lead was made thicker: 10 cm. In addition, the back side polyethylene was changed to concrete to remove the bypass for gammas. It was shown that the redesigned shielding effectively stops all gamma heading for the z direction without any noticeable leak.

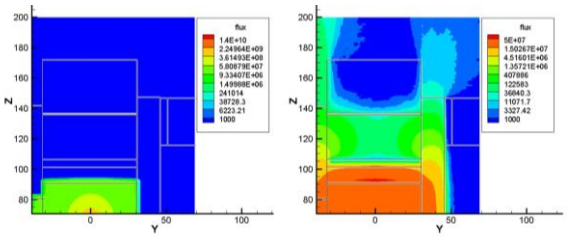

Fig. 7. Distribution of neutron and gamma flux with the original top shielding above the monochromator

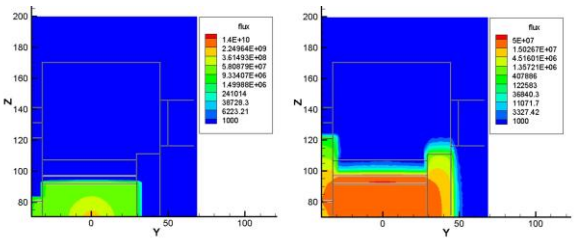

Fig. 8. Distribution of neutron and gamma flux with revised top shielding above the monochromator

2.3.3 Shielding below the monochromator

The redesign of the monochromator shielding required thinner concrete shielding below the monochromator. It was 31 cm before, but became 25 cm. Thanks to the denser concrete, however, the shielding was more effective.as compared in figures 9 and 10.

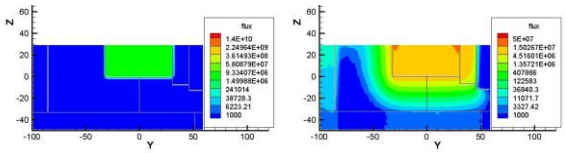

Fig. 9. Distribution of neutron and gamma flux below the monochromator with the original geometry

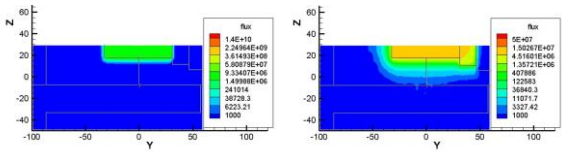

Fig. 10. . Distribution of neutron and gamma flux below the monochromator with the modified geometry

3. Conclusions

The monochromator shielding blocks are studied by MCNP calucations to reduce the radiation in the current redesign effort. We could identify where the most of the leaks occur and decrease them by placing lead and stainless steel on top of the polyethylene of the segmented shielding parts. Even with the thinner concrete shielding below the monochromator, gamma was more effectively shielded by using the higher density concrete.

While the current study warrants the shielding effectiveness of the redesigned concrete shielding, there are more shielding parts to study such as the beam dump, the lead block called “the mustache” after the segmented shielding and the collimator box embedded in it. This requires more accurate treatment of the neutron beam and the consideration must be given to 1) the neutron beam flux that was filtered, and thus greatly reduced, by the neutron velocity selector and 2) the reflected neutron beam by the Bragg’s law by the monochromator. It will be the focus of the future study.

REFERENCES

[1] J. M. Ryu. K. P. Hong, J. M. S. Park, Y. H. Choi, and K. H. Lee, Shielding Design Optimization of the HANARO Cold Neutron Triple-axis Spectrometer, The Korean Association for Radiation Protection, Vol.39, No. 1 p. 21-29, 2014.
[2] J. M. Ryu. K. P. Hong, J. M. S. Park, Y. H. Choi, and K. H. Lee, Shielding Design of Cold Neutron Triple-axis

Spectrometer using MCNP6, Transactions of the Korean Nuclear Society Spring Meeting, 2014.
[3] J. M. S. Park, J. M. Ryu, B. Jeon, J. Kim and B. S. Seong, Status of the Triple-Axis Spectrometer Modifications at HANARO, The 15th Japan-Korea Meeting on Neutron Science, 2016.
[4] J. M. S. Park, and J. M. Ryu, The first McStas Simulation of the HANARO Cold Neutron Triple-Axis Spectrometer, 2015 International HANARO Symposium.